Particuology 9 (2011) 465–470

Contents lists available at ScienceDirect

Particuology

journal homepage: www.elsevier.com/locate/partic

Effects of bimetallic catalysts on synthesis of nitrogen-doped carbon nanotubes as nanoscale energetic materials

Hao Liu[a], Yong Zhang[a], Ruying Li[a], Xueliang Sun[a,*], Hakima Abou-Rachid[b,**]

[a] Department of Mechanical and Materials Engineering, University of Western Ontario, London, ON N6A 5B9, Canada
[b] Defense Research & Development Canada, 2459 Boulevard PieXI Nord, Québec, QC G3J 1X5, Canada

ARTICLE INFO

Article history:
Received 13 December 2010
Received in revised form 6 February 2011
Accepted 21 February 2011

Keywords:
Nitrogen doped carbon nanotubes
Chemical vapor deposition
Bimetallic catalyst

ABSTRACT

Well aligned nitrogen-doped carbon nanotubes (CN_x-NTs), as energetic materials, are synthesized on a silicon substrate by aerosol-assisted chemical vapor deposition. Tungsten (W) and molybdenum (Mo) metals are respectively introduced to combine with iron (Fe) to act as a bimetallic co-catalyst layer. Correlations between the composition and shape of the co-catalyst and morphology, size, growth rate and nitrogen doping amount of the synthesized CN_x-NTs are investigated by secondary and backscattered electron imaging in a field emission scanning electron microscope (FESEM) and X-ray photoelectron spectrometer (XPS). Compared to pure iron catalyst, W–Fe co-catalyst can result in lower growth rate, larger diameter and wider size distribution of the CN_x-NTs; while incorporation of molybdenum into the iron catalyst layer can reduce the diameter and size distribution of the nanotubes. Compared to the sole iron catalyst, Fe–W catalyst impedes nitrogen doping while Fe–Mo catalyst promotes the incorporation of nitrogen into the nanotubes. The present work indicates that CN_x-NTs with modulated size, growth rate and nitrogen doping concentration are expected to be synthesized by tuning the size and composition of co-catalysts, which may find great potential in producing CN_x-NTs with controlled structure and properties.

1. Introduction

Polymeric nitrogen was theoretically predicted by Mailhiot, Yang, and McMahan (1992) and experimentally synthesized by Eremets, Gavriliuk, Trojan, Dzivenko, and Boehler (2004), but under high temperature and pressure, both not desirable for its practical application as an energetic material. So far, no polymeric nitrogen has been synthesized stable at ambient temperature and pressure. However, a recent theoretical study showed that when a polymeric nitrogen chain is encapsulated in a carbon nanotube (CNT), it will be stable at ambient pressure and room temperature (Abou-Rachid, Hu, Timoshevskii, Song, & Lussier, 2008), thus making CNT promising in preparing nanoscale energetic materials. Carbon nanotubes are known to have unique electrical (Langer et al., 1996), mechanical (Rafii-Tabar, 2008; Yu, Files, Arepalli, & Ruoff, 2000) and thermal properties (Rafii-Tabar, 2008), and they have attracted considerable interest due to their potential applications in nanoelectronics (Fennimore et al., 2003), in sensors (Huang et al., 2002) and as catalyst supports (Villers, Sun, Serventi, Dodelet, & Desilets, 2006). There has been a significant number of reports on the synthesis of single-walled and multi-walled CNTs using Fe, Co, or Ni catalysts (Liu et al., 2008; Sun et al., 2007). Efficient catalysts should possess long activation life, high selectivity and immunity from contamination (Harutyunyan et al., 2007). Chemical poisoning or carbon coating (Zhou et al., 2003), thermal sintering (Cantoro et al., 2006) and solid-state deteriorations, such as the formation of silicide with silicon substrate at high temperature (Jung et al., 2003), are the common factors that lead to reduction of catalytic activity.

As an alternative, the use of metal alloy catalysts such as Fe–Co, Co–Mo and Fe–Ni has been found to improve the growth of CNTs (Biris et al., 2008; Cui, Wu, Wu, Tian, & Chen, 2008; Niu & Fang, 2008; Saito et al., 2005; Sugime, Noda, Maruyama, & Yamaguchi, 2009), because catalyst activity is significantly enhanced by the synergetic effect of the metals involved (Harutyunyan et al., 2007; Alvarez, Kitiyanan, Borgna, & Resasco, 2001). In addition, aggregation of catalyst particles can be prevented by the presence of more than one metal species (Tang et al., 2001). For example, the addition of Mo in mechanical alloying of powder Fe and C mixture promotes solid-state reactions even at a low Mo concentration by forming

* Corresponding author. Fax: +1 519 661 3020.
** Corresponding author. Fax: +1 418 844 4646.
E-mail addresses: xsun@eng.uwo.ca (X. Sun), hakima.abou-rachid@drdc-rddc.gc.ca (H. Abou-Rachid).

1674-2001/$ – see front matter © 2011 Chinese Society of Particuology and Institute of Process Engineering, Chinese Academy of Sciences. Published by Elsevier B.V. All rights reserved.
doi:10.1016/j.partic.2011.02.009

ternary phases (Omuro, Miura, & Ogawa, 1994). For this case, even the size and diameter distribution of the carbon nanotubes can be modulated in a controlled way.

On the other hand, the use of co-catalyst instead of sole metals provides additional degrees of freedom, such as fractions of the metal species, which have chemical and thermodynamic advantages. The chemical advantages arise since the fractions of constituent species can be tailored to enhance catalytic performance of the catalysts (Alvarez et al., 2001). It has been reported that the presence of the phase $Fe_2(MoO_4)_3$ can lead to the formation of smaller metallic clusters, which is favorable for the growth of SWCNTs (Lamouroux, Serp, Kihn, & Kalck, 2007). The thermodynamic advantages are revealed since vapor–liquid–solid model has been considered as the most possible mechanism of CNT growth (Harutyunyan et al., 2007; Gorbunov, Jost, Pompe, & Graff, 2002). Metallic nanoparticles are very efficient catalysts at their liquid or viscous state, probably because of considerable carbon bulk diffusion in these phases, as compared to surface or subsurface diffusion. Melting point of the catalyst is reduced by adding alloying components. Hence, the composition of catalyst nanoparticles could be tailored to enhance the yield and quality of CNTs by moving the liquid line of the alloy below the synthesis temperature.

Regular CNTs have been extensively investigated in the presence of a co-catalyst, though co-catalyst effect has been seldom discussed on the synthesis of CN_x-NTs even though some binary metal particles were indeed employed (Kudashov et al., 2004; Lim et al., 2006; Tao et al., 2007). As for the growth of CN_x-NTs, nitrogen diffusion within the catalyst particles is very critical (Srivastava, Vankar, & Kumar, 2006). As discussed above, co-catalyst can modulate the diffusions within catalyst particles. Therefore, a comprehensive study in this field is necessary in terms of correlation between catalyst composition, size and nitrogen doping of CNTs.

In the present work, molybdenum and tungsten are respectively alloyed to iron as co-catalyst elements. Their effects on the morphology, size, growth rate and nitrogen content of the CN_x-NTs are investigated.

2. Experimental

Aerosol-assisted chemical vapor deposition (AACVD) was used for the growth of CN_x-NTs, as has already been reported (Zhang et al., 2009), using two argon inlets and one hydrogen inlet. One argon inlet was used for carrier gases flowing through the aerosol solution and then carrying the aerosol into the reaction chamber. An additional argon inlet enables diluting the obtained aerosol mixture. Hydrogen was introduced into the reaction chamber from the hydrogen inlet. Acetonitrile (CH_3CN) which serves as both carbon and nitrogen sources was placed inside a sonication generator and thermostated during synthesis at room temperature by cooling water.

A silicon wafer with a 600 nm-thick SiO_2 layer was used as the substrate. Fe and W or Mo were sputtered onto the silicon wafer working as catalyst in the growth of CN_x-NTs. Experiments were performed at atmospheric pressure as follows. The pretreated silicon substrate was placed in a ceramic boat inside the reaction chamber. The furnace was heated to 870 °C, after a 20 min expulsion of air in the chamber by 400 sccm argon. As soon as the target temperature was reached, aerosol droplets were produced by ultrasonication with a frequency of 850 kHz and transported by argon gas at a flow rate of 1500 sccm. At the same time, hydrogen was introduced at a flow rate of 1100 sccm as the reaction gas to reduce the catalyst precursor to form active Fe^0 catalyst. Through another inlet, argon with a gas flow rate of 900 sccm was admitted to dilute the aerosol gas in the reaction chamber. At the end of the experiment which lasted for 30 min, the aerosol generator and furnace were turned off. Gases were kept passing through the reactor until the furnace cooled down to room temperature.

The samples were characterized by using a Hitachi S-4800 field-emission scanning electron microscope (SEM) operated at 5.0 kV, a Philips CM10 transmission electron microscope (TEM) operated at 80 kV and a Multilab 3000 XPS system of Thermo VG Scientific. XPS data were collected with a dual anode X-ray source using Mg K irradiation with 1253.6 eV. Binding energies were measured using a hemispherical energy analyzer with fixed pass energy of 50 eV with an energy resolution of about 1.1 eV. All data were analyzed using an XPS data analysis software, Advantage version 3.99, by Thermo VG Scientific. Fittings of the peaks were performed by using Gaussian–Lorentzian product function and Shirley background algorithm. Sensitivity factors were also taken into account during the quantitative analysis.

3. Results and discussion

Fig. 1 shows the SEM images of CN_x-NTs synthesized by different catalyst layers. The length, diameter and shape of catalyst of the tubes noticeably change with the additive of W or Mo catalyst layers. Fig. 1(a) shows the diameters of the CN_x-NTs synthesized without any co-catalyst layer are mainly in the range of 30–90 nm, and 170 μm in length, as shown in low magnification image at lower right corner. An SEM image using backscattered electron imaging at the upper right corner shows the cone-like structure of the catalysts.

When W is employed as a co-catalyst material, the diameter distribution is enlarged to 20–130 nm, as shown in Fig. 1(b). CN_x-NTs with larger diameters, even beyond 200 nm, are also observed when W is employed as a co-catalyst material. Meanwhile, from our observations of the low magnification SEM image in the lower right corner, the growth rate of these tubes is greatly reduced with the addition of W catalyst layer, and the length of the tubes is reduced to 100 μm. The restriction of the growth rate of CN_x-NTs with addition of W co-catalyst can be attributed to the decreased diffusion of carbon atoms in W, because W is much less active in producing tubular carbonaceous products (Qian, Qi, & Liu, 2007). Another remarkable phenomenon with the addition of W co-catalyst layer is the change of shape of the catalysts shown in the backscattered electron image at the upper right corner, which will be discussed in detail later.

Similar experimental study has been conducted using Mo as a co-catalyst material. The secondary and backscattered electron images of the CN_x-NTs synthesized with Mo co-catalyst, in Fig. 1(c), show smaller diameter of CN_x-NTs. The high-magnification SEM image shows the diameter of the tubes is around 20 nm. On the other hand, the growth of the CN_x-NTs is slightly enhanced possibly due to the improved activity of the co-catalyst by the addition of Mo (Delzeit et al., 2001). The length of the CN_x-NTs increases to 190 μm. The thinner diameter and narrower size distribution of the nanotubes can be attributed to the formation of Fe–Mo alloy or inter-metallic compounds, which result in the formation of small and well-dispersed metallic clusters due to the stabilizing effect of molybdenum (Lamouroux et al., 2007). The enhanced growth of CN_x-NTs when Mo is employed can be attributed to the reduction of melting point resulting from the addition of small fraction of Mo to Fe (Kottcamp Jr. et al., 1992). Similar to the case using Fe–W co-catalyst, the addition of Mo to Fe also affects the shape of the catalyst, leading to the variation of the shape of catalyst from cone shape to rod shape, as shown in the backscattered SEM image.

XPS analysis is carried out to study the co-catalyst effect on nitrogen content of CN_x-NTs. Fig. 2 shows, separately, the XPS

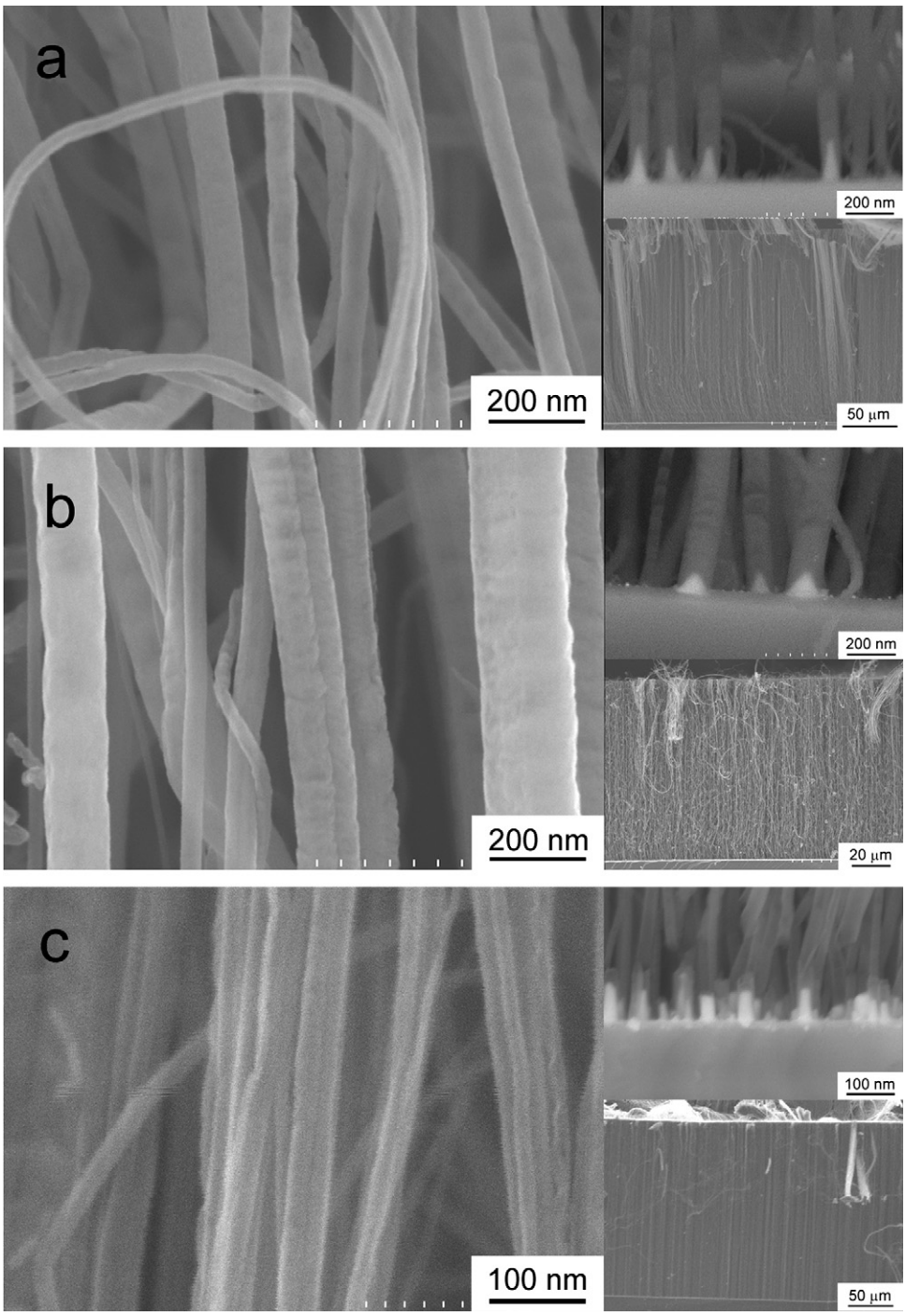

Fig. 1. SEM images of CN_x-NTs synthesized with (a) Fe, (b) Fe/W and (c) Fe/Mo catalyst layers. In each image, the bigger left image is the high magnification SEM image, the upper right corner is the backscattered electron image and the lower right corner is low magnification SEM image.

spectra taken from the CN_x-NTs synthesized by Fe, Fe/W and Fe/Mo catalyst layers. From the survey scan of the CN_x-NTs in Fig. 2(a), it is observed that the nitrogen content, which is defined as N/C at % and estimated by the area ratio of the nitrogen and carbon peaks (Nath, Satishikumar, Gobindaraj, Vinod, & Rao, 2000), decreases from 1.3% to 0.4% as W is added as a co-catalyst element, and increases to 1.7% when Mo is added as a co-catalyst element. Generally the nitrogen content inside carbon nanotubes correlates closely to the nature of the catalyst particles (Bethune et al., 1993). It has been reported that higher growth rate of CNTs favors the incorporation of nitrogen into the nanotube walls (Kudashov et al., 2004). In our work, addition of molybdenum into the iron catalyst promotes the growth rate of the nanotubes while addition of tungsten decreases the growth rate. This could be responsible for the nitrogen difference between the nanotubes catalyzed by iron–molybdenum and iron–tungsten particles. In this case, diffusion and segregation behavior of nitrogen and carbon in the catalysts with different composition needs to be considered. The high resolution N 1s spectra of these CN_x-NTs synthesized with Fe, Fe/W and Fe/Mo are shown separately in Fig. 2(b)–(d). The asymmetric N 1s spectra indicate the existence of several components. Although signal intensity ratio of different nitrogen species varies depending on the

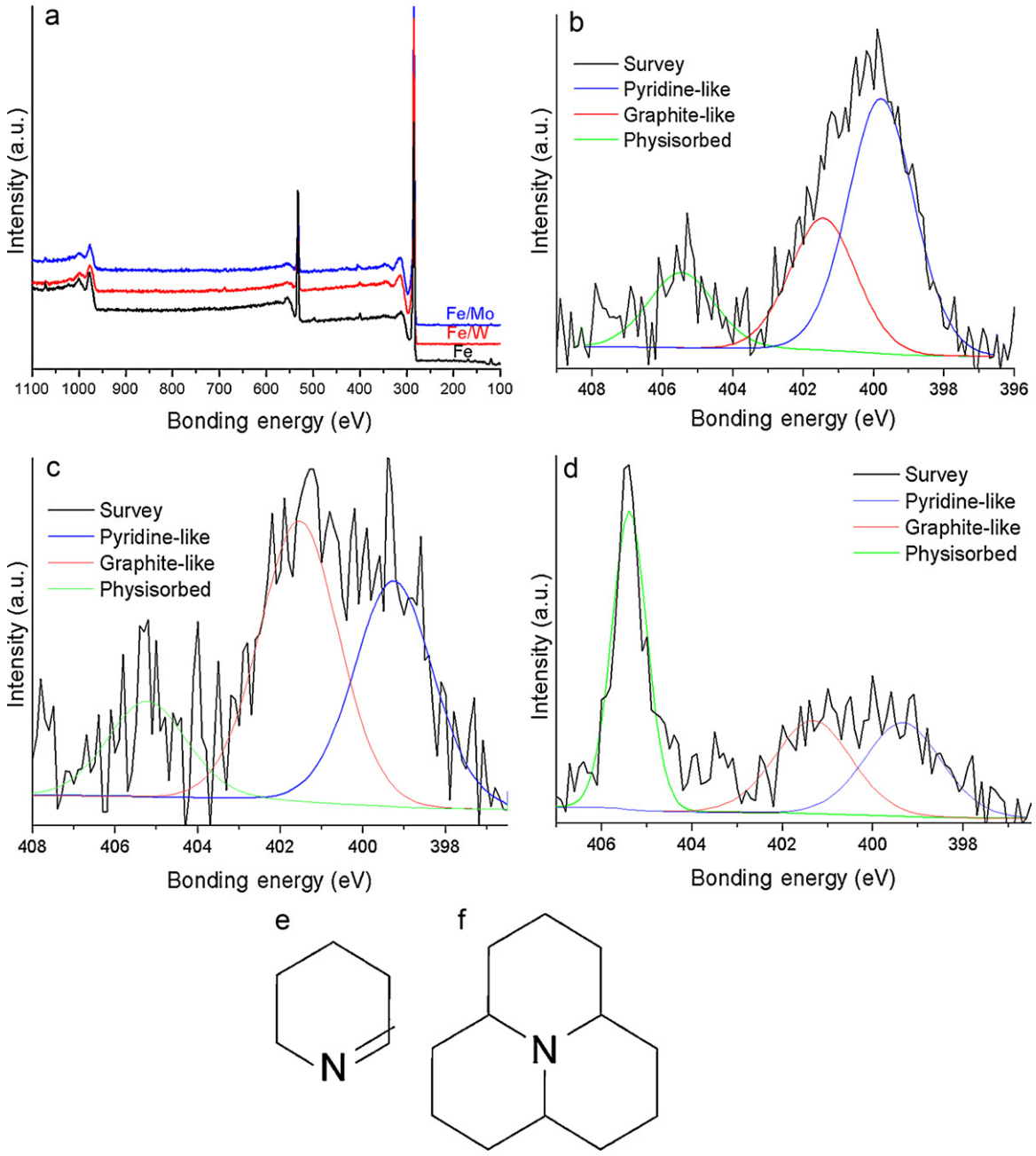

Fig. 2. (a) Full survey of XPS results of CN_x-NTs; high resolution XPS results of CN_x-NTs using catalyst layer of: (b) Fe, (c) Fe/W, and (d) Fe/Mo; nitrogen species found in CN_x-NTs: (e) pyridine-like nitrogen, and (f) graphite-like nitrogen.

catalyst employed, and spectrum peaks of the nanotubes grown from Fe–W catalyst are affected by background noise, the spectra can be fitted into three peaks. The peaks around 399.5, 401.5 and 405 eV correspond to pyridine-like nitrogen, graphite-like nitrogen and physisorbed nitrogen, respectively (Liu et al., 2010). Pyridine-like nitrogen atoms contribute to the π system with a pair of π electrons and only bonded to two C atoms (C–N=C), as shown in Fig. 2(e), while the graphite-like nitrogen corresponds to highly coordinated N atoms substituting inner C atoms on the graphite layers, as shown in Fig. 2(f).

To investigate the chemical environment of the incorporated N species systematically, N 1s XPS spectra are summarized in Table 1. It is worthy to know that the fraction of different nitrogen species varies as the catalyst composition changes. Pyridine-like nitrogen is dominant with iron as the sole catalyst. But the nitrogen changes to a more stable format, i.e. graphite-like nitrogen when W is employed as co-catalyst. However, when Mo is used as the co-catalyst material, the dominant nitrogen species changes to physisorbed nitrogen, indicating that larger amount of molecular nitrogen is encapsulated inside the compartments and interlayers of the CN_x-NTs, as is similar to the previous report (Choi et al., 2005).

Table 1
Nitrogen incorporation profile within the CN_x-NT grown from different co-catalysts.

Catalyst	Nitrogen content (%)	Pyridine-like (%)	Graphite-like (%)	Physisorbed (%)
Fe	1.3	55.2	28.5	16.3
Fe/W	0.4	37.6	46.6	15.9
Fe/Mo	1.7	29.2	28.9	41.9

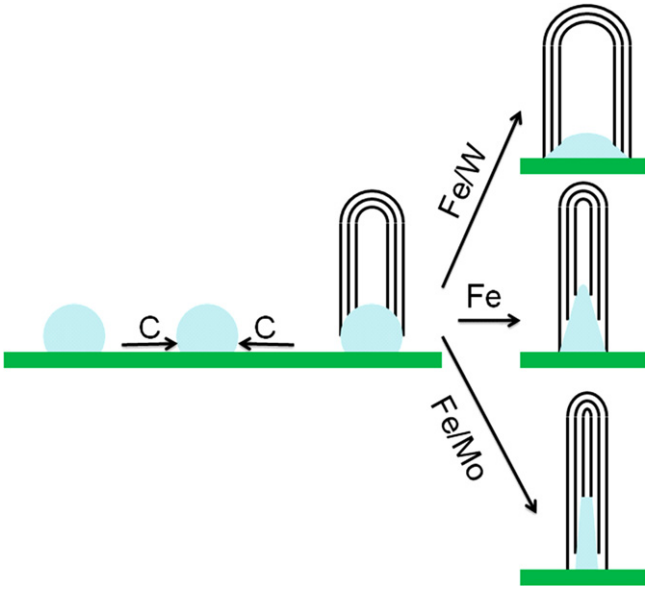

Fig. 3. Schematic growth diagram of the CN_x-NTs using Fe, Fe/W and Fe/Mo catalysts.

Fig. 3 shows schematically the growth processes of CN_x-NTs, focusing on the shape difference of the catalyst particles for different catalyst combinations. Before carbon gas was introduced into the chamber, small particles were formed on the surface of the substrate upon elevating the temperature. When carbon source was introduced into the chamber, hydrocarbon molecules were dissociated by the catalysts. The carbon species dissolved and saturated in the catalysts, and precipitated from the catalyst, led to the formation of tubular structures. Because of strong interaction between the catalyst and the substrate, the growth of the nanotubes followed a base-growth mode. At the nucleation stage of the CNTs, the initially formed inner tube walls would compress and encapsulate the liquid or partly liquid catalyst. To release the stress, the catalyst tended to be deformed into certain shape to match the innermost wall of the nanotube. Meanwhile, the interfacial tension between the liquid catalyst and the substrate prevented the deformation, forcing the shape of the catalyst to change to a cone-like structure (Lin et al., 2007). However, as the W co-catalyst element was added, the ratio of height to diameter of the catalyst decreased greatly. It has been reported that the hardness of Fe is elevated with the addition of W (Donten, Cesiulis, & Stojet, 2000), and the catalyst was harder to be shaped. This explains the reason why the shape of the catalyst changes with the increase of W content. On the other hand, when Mo is employed as a co-catalyst element, the catalysts change from the cone shape to a rod shape due to a similar reason.

4. Conclusion

A detailed investigation of the effects of co-catalyst on the growth of CN_x-NTs has been comprehensively conducted in the present work. W and Mo were introduced into the catalyst layer to form co-catalyst compositions with Fe. The diameter of CN_x-NTs increases and the growth rate of CN_x-NTs decreases with the introduction of W catalyst layer. The W catalyst layer can also broaden the distribution of diameters of CN_x-NTs. The Mo catalyst layer, however, has an opposite effect on the diameter of CN_x-NTs as compared to W. The diameter of CN_x-NTs decreases with the addition of Mo catalyst layer, while the growth rate of CN_x-NTs is enhanced at the same time. The shape of our catalyst is also observed changing with the addition of either the W or Mo catalyst layer. Co-catalyst also has the effect of incorporation of nitrogen. Compared to the sole iron catalyst, Fe–W catalyst impedes nitrogen doping while Fe–Mo catalyst promotes the incorporation of nitrogen into the nanotubes. According to the present work, the size, growth and nitrogen doping concentration of CN_x-NTs are expected to be modulated by tuning the size and composition of co-catalysts, which may find great potential in producing CN_x-NTs with controlled structure and properties.

References

Abou-Rachid, H., Hu, A., Timoshevskii, V., Song, Y., & Lussier, L.-S. (2008). Nanoscale high energetic materials: A polymeric nitrogen chain N_8 confined inside a carbon nanotube. *Physical Review Letters*, *100*, 196401.

Alvarez, W. E., Kitiyanan, B., Borgna, A., & Resasco, D. E. (2001). Synergism of Co and Mo in the catalytic production of single-wall carbon nanotubes by decomposition of CO. *Carbon*, *39*, 547–558.

Bethune, D. S., Kiang, C. H., de Vries, M. S., Gorman, G., Savoy, R., Vazquez, J., et al. (1993). Cobalt-catalyzed growth of carbon nanotubes with single-atomic-layer walls. *Nature*, *363*, 605–607.

Biris, A. R., Li, Z., Dervishi, E., Lupu, D., Xu, Y., Saini, V., et al. (2008). Effect of hydrogen on the growth and morphology of single wall carbon nanotubes synthesized on a Fe–Mo/MgO catalytic system. *Physics Letters A*, *372*, 3051–3057.

Cantoro, M., Hofmann, S., Pisana, S., Scardaci, V., Parvez, A., Ducati, C., et al. (2006). Catalytic chemical vapor deposition of single-wall carbon nanotubes at low temperature. *Nano Letters*, *6*, 1107–1112.

Choi, H. C., Bae, S. Y., Jang, W. S., Park, J., Song, H. J., Shin, H. J., et al. (2005). Release of N_2 from the carbon nanotubes via high-temperature annealing. *The Journal of Physical Chemistry B*, *109*, 1683–1688.

Cui, Y., Wu, X., Wu, H., Tian, Y., & Chen, Y. (2008). Optimization of synthesis condition for carbon nanotubes by chemical vapor deposition on Fe–Ni–Mo/MgO catalyst. *Materials Letters*, *62*, 3878–3880.

Delzeit, L., Chen, B., Cassell, A., Stevens, R., Nguyen, C., & Meyyappan, M. (2001). Multilayered metal catalysts for controlling the density of single-walled carbon nanotube growth. *Chemical Physics Letters*, *348*, 368–374.

Donten, M., Cesiulis, H., & Stojet, Z. (2000). Electrodeposition and properties of Ni–W, Fe–W and Fe–Ni–W amorphous alloys: A comparative study. *Electrochimica Acta*, *45*, 3389–3396.

Eremets, M. I., Gavriliuk, A. G., Trojan, I. A., Dzivenko, D. A., & Boehler, R. (2004). Single-bonded cubic form of nitrogen. *Nature Materials*, *3*, 558–563.

Fennimore, A. M., Yuzvinsky, T. D., Han, W.-Q., Fuhrer, M. S., Cumings, J., & Zettl, A. (2003). Rotational actuators based on carbon nanotubes. *Nature*, *424*, 408–410.

Gorbunov, A., Jost, O., Pompe, W., & Graff, A. (2002). Solid–liquid–solid growth mechanism of single-walled carbon nanotubes. *Carbon*, *40*, 113–118.

Harutyunyan, A. R., Mora, E., Tokune, T., Bolton, K., Rose, A., Jiang, A., et al. (2007). Hidden features of the catalyst nanoparticles favorable for single-walled carbon nanotube growth. *Applied Physics Letters*, *90*, 163120.

Huang, W., Taylor, S., Fu, K., Lin, Y., Zhang, D., Hanks, T. W., et al. (2002). Attaching proteins to carbon nanotubes via diimide-activated amidation. *Nano Letters*, *2*, 311–314.

Jung, Y. J., Wei, B. Q., Vajtai, R., Ajayan, P. M., Homma, Y., Prabhakaran, K., et al. (2003). Mechanism of selective growth of carbon nanotubes on SiO_2/Si patterns. *Nano Letters*, *3*, 561–564.

Kottcamp Jr., E. H. ASM handbook: Volume 3: Alloy Phase Diagram, US, 1992, ISBN 0-87170-381-5.

Kudashov, A. G., Okotrub, A. V., Bulusheva, L. G., Asanov, I. P., Shibin, Y. V., Yudanov, N. F., et al. (2004). Influence of Ni–Co catalyst composition on nitrogen content in carbon nanotubes. *The Journal of Physical Chemistry B*, *108*, 9048–9053.

Lamouroux, E., Serp, P., Kihn, Y., & Kalck, P. (2007). Identification of key parameters for the selective growth of single or double wall carbon nanotubes on $FeMo/Al_2O_3$ CVD catalysts. *Applied Catalysis A*, *323*, 162–173.

Langer, L., Bayot, V., Grivei, E., Issi, J.-P., Heremans, J. P., Olk, C. H., et al. (1996). Quantum transport in a multiwalled carbon nanotube. *Physical Review Letters*, *76*, 479–482.

Lim, S. H., Elim, H. I., Gao, X. Y., Wee, A. T. S., Ji, W., Lee, J. Y., et al. (2006). Electronic and optical properties of nitrogen-doped multiwalled carbon nanotubes. *Physical Review B*, *73*, 045402.

Lin, M., Tan, J. P. Y., Boothroyd, C., Loh, K. P., Tok, E. S., & Foo, Y.-L. (2007). Dynamical observation of bamboo-like carbon nanotube growth. *Nano Letters*, *7*, 2234–2238.

Liu, H., Zhang, Y., Arato, D., Li, R., Mérel, P., & Sun, X. (2008). Aligned multi-walled carbon nanotubes on different substrates by floating catalyst chemical vapor deposition: Critical effects of buffer layer. *Surface and Coatings Technology*, *202*, 4114–4120.

Liu, H., Zhang, Y., Li, R., Sun, X., Désilets, S., Abou-Rachid, H., et al. (2010). Structural and morphological control of aligned nitrogen-doped carbon nanotubes. *Carbon*, *48*(5), 1498–1507.

Mailhiot, C., Yang, L. H., & McMahan, A. K. (1992). Polymeric nitrogen. *Physical Review B*, *46*, 14419–14435.

Nath, M., Satishikumar, B. C., Gobindaraj, A., Vinod, C. P., & Rao, C. N. R. (2000). Production of bundles of aligned carbon and carbon–nitrogen nanotubes by the

pyrolysis of precursors on silica-supported iron and cobalt catalysts. *Chemical Physics Letters*, *322*(5), 333–340.
Niu, Z., & Fang, Y. (2008). Effect of temperature for synthesizing single-walled carbon nanotubes by catalytic chemical vapor deposition over Mo–Co–MgO catalyst. *Materials Research Bulletin*, *43*, 1393–1400.
Omuro, K., Miura, H., & Ogawa, H. (1994). Amorphization in iron–carbon systems with transition metals by mechanical alloying. *Materials Science and Engineering: A*, *181–182*, 1281–1284.
Qian, C., Qi, H., & Liu, J. (2007). Effect of tungsten on the purification of few-walled carbon nanotubes synthesized by thermal chemical vapor deposition methods. *The Journal of Physical Chemistry C*, *111*, 131–133.
Rafii-Tabar, H. (2008). *Computational physics of carbon nanotubes*. Cambridge: Cambridge University Press.
Saito, T., Ohshima, S., Xu, W.-C., Ago, H., Yumura, M., & Iijima, S. (2005). Size control of metal nanoparticle catalysts for the gas-phase synthesis of single-walled carbon nanotubes. *The Journal of Physical Chemistry B*, *109*, 10647–10652.
Srivastava, S. K., Vankar, V. D., & Kumar, V. (2006). Growth and microstructures of carbon nanotube films prepared by microwave plasma enhanced chemical vapor deposition process. *Thin Solid Films*, *515*(4–5), 1552–1560.
Sugime, H., Noda, S., Maruyama, S., & Yamaguchi, Y. (2009). Multiple "optimum" conditions for Co–Mo catalyzed growth of vertically aligned single-walled carbon nanotube forests. *Carbon*, *47*, 234–241.
Sun, X., Li, R., Stansfield, B., Dodelet, J. P., Menard, G., & Desilets, S. (2007). Controlled synthesis of pointed carbon nanotubes. *Carbon*, *45*(4), 732–737.
Tang, S., Zhong, Z., Xiong, Z., Sun, L., Liu, L., Lin, J., et al. (2001). Controlled growth of single-walled carbon nanotubes by catalytic decomposition of CH_4 over Mo/Co/MgO catalysts. *Chemical Physics Letters*, *350*, 19–26.
Tao, X. Y., Zhang, X. B., Sun, F. Y., Cheng, J. P., Liu, F., & Luo, Z. Q. (2007). Large-scale CVD synthesis of nitrogen-doped multi-walled carbon nanotubes with controllable nitrogen content on a $Co_xMg_{1-x}MoO_4$ catalyst. *Diamond and Related Materials*, *16*, 425–430.
Villers, D., Sun, S. H., Serventi, A. M., Dodelet, J. P., & Desilets, S. (2006). Characterization of Pt nanoparticles deposited onto carbon nanotubes grown on carbon paper and evaluation of this electrode for the reduction of oxygen. *The Journal of Physical Chemistry B*, *110*(51), 25916–25925.
Yu, M. F., Files, B. S., Arepalli, S., & Ruoff, R. S. (2000). Tensile loading of ropes of single wall carbon nanotubes and their mechanical properties. *Physical Review Letters*, *84*, 5552–5555.
Zhang, Y., Li, R., Liu, H., Sun, X., Merel, P., & Desilet, S. (2009). Integration and characterization of aligned carbon nanotubes on metal/silicon substrates and effects of water. *Applied Surface Science*, *255*, 5003–5008.
Zhou, Z., Ci, L., Chen, X., Tang, D., Yan, X., Liu, D., et al. (2003). Controllable growth of double wall carbon nanotubes in a floating catalytic system. *Carbon*, *41*, 337–342.